



Thermodynamic and Global Reactivity Parameter Indices for Catechol Based Dipodal Complex with Trivalent Heavy Metal Ions

AMARDEEP¹, VIJAY DANGI^{1,*}, PRAMOD KUMAR¹, MEENAKSHI¹, MINATI BARAL², TARUNA SHEORAN³ and BRAHAMDUTT ARYA^{4,5,*}

¹Department of Chemistry, Baba Mastnath University, Rohtak-124021, India

²Department of Chemistry, National Institute of Technology, Kurukshetra-136119, India

³Department of Bio and Nano Technology, Guru Jambheshwar University of Science and Technology, Hisar-125001, India

⁴Department of Higher Education, Shiksha Sadan, Sector-5, Panchkula-134114, India

⁵Y & Y Nanotech Solutions Private Limited, Rohtak-124001, India

*Corresponding authors: E-mail: 91dangi@gmail.com; brahm.chem@gmail.com

Received: 30 March 2024;

Accepted: 30 April 2024;

Published online: 29 June 2024;

AJC-21671

Heavy metal ions are of major concern due to their potential toxicity to humans and environment. Schiff base biomimetic ligands have shown immense potential to mitigate the heavy metal ions toxicity. In present study, the thermodynamic and stability parameters for catechol based Schiff base ligand MEC-trivalent metal ions (Al^{3+} , Cr^{3+} and Fe^{3+}) complexes (where MEC = N_1, N_3 -bis(2-((Z)-2,3-dihydroxybenzylidene)amino)ethyl)malonamide) were investigated using DFT and TD-DFT approaches. Further, in order to propose the involvement of these metal-ligand complexes in various applications, the conceptual density functional theory analysis were also conducted.

Keywords: DFT, Schiff base, Conceptual DFT, Catechol, Heavy metal, Toxicity, Remediation.

INTRODUCTION

Heavy metals such as aluminum, chromium and iron play a major role as pollutants in the environment [1]. The sources of these metals include industrial activities like mining, smelting and manufacturing, which release them into the ecosystem and lead to their accumulation in soil, water and air [2]. Iron, aluminum and chromium are ubiquitous in the environment and play crucial roles in various industrial applications. However, their toxicity poses risks to human health and ecological stability when present in excessive amounts or in certain toxic forms [1,3]. Nevertheless, an excessive amount of iron can be harmful, since it can result in a condition known as hemochromatosis or iron overload condition [4]. Further, accumulation of iron in organs and tissues can cause several serious health concerns, such as diabetes, cardiac problems and liver disease [5]. Moreover, high concentration of iron is among the chief contributors to some environmental issues like eutrophication of water, causing severe detrimental effect on aquatic life by affecting the quality of water [6].

Similarly, exposure to high concentration of aluminium, can induce certain neurological toxicity in humans and can be

connected to various deadly disease like Alzheimer's and certain types of cancers [7,8]. Further, elevated concentration of aluminum can project serious environment issue by affecting the soil and water. It has also been found that aluminum toxicity can severely affect the aquatic life and forest ecosystems by affecting pH levels and causing toxic effects on fish and plant roots [9]. On the other hand, chromium being a chief source of industrial pollutant, can exist in a number of different oxidation states, with trivalent chromium being an important nutrient and hexavalent chromium being extremely hazardous and carcinogenic [10]. In addition to being associated with the development of respiratory system malignancies, direct contact with hexavalent chromium has been linked to skin irritations and ulcers [11]. It is a factor that contributes to the degradation of ecosystems and has negative effects on the biological and ecological species that live in them [12].

In the realm of environmental and public health management, the task of reducing the toxicity of heavy metals like iron, chromium and aluminium is a challenging one, but it is imperative that it be accomplished. In spite of the fact that these metals are found in nature and play an important role in a variety of biological processes, their presence in excessive amounts

as pollutants can have negative consequences for both the environment and human health.

A number of efforts have been made by different research groups to mitigate the contamination of these heavy metal ions. Application of organic Schiff base ligands for effective detection and capture of heavy metal ions have attracted numerous scientific interest [13,14]. The main advantage of utilizing Schiff base ligand for heavy metal pollution mitigation is that the metal-ligand complex that is left over after the removal of heavy metal ions can be used in a variety of ways like catalytic activities, fabrication of optical devices, dyes, development of novel pharmaceutically active molecules, biological activities and in various nanotechnology based applications like drug delivery, biosensors and photodynamic therapy [13]. Recently, we have reported the experimental complex formation capabilities of Schiff base ligand (MEC) for effective and efficient detection and complexation of trivalent metal ions, in a pH dependent manner [15].

In present study, we have investigated the thermodynamic and stability studies for MEC-Al³⁺, MEC-Cr³⁺ and MEC-Fe³⁺ complexes using DFT and TD-DFT analysis (where MEC = N₁,N₃-bis(2-(((Z)-2,3-dihydroxybenzylidene)amino)ethyl)-malonamide) (Fig. 1). Further, in order to access the potential for employment of these metal-ligand complexes in certain applications, we have critically analyzed the global reactivity parameter indices using conceptual density functional theory. Further, the molecular electrostatic surface potential for analyzing the preferred sites of electrophilic and nucleophilic attacks in the organic transformation were also discussed.

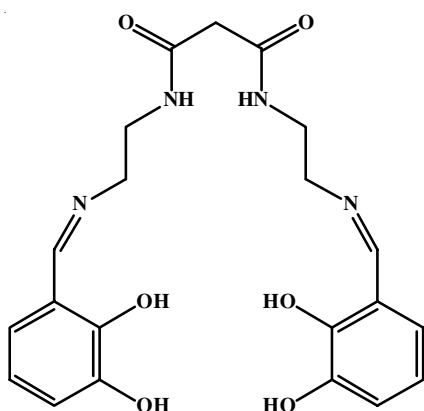


Fig. 1. Chemical structure of Schiff base ligand, N₁,N₃-bis(2-(((Z)-2,3-dihydroxybenzylidene)amino)ethyl)malonamide) (MEC)

EXPERIMENTAL

Molecular modeling: All the calculations were performed on 11th Gen Intel(R) Core (TM) i7-11700K @ 3.40 GHz system using Gaussian 09 software [16]. In present study, the density functional theory (DFT) was employed for optimizing the proposed molecules. Further, in order to access the various structural characteristics of metal complexes in the gas phase, the B3LYP hybrid parameter was employed using computational calculations [17]. In order to confirm that the structures are real minima *i.e.* with minimum energies, vibrational frequency

calculations were carried out at the same level of theory, after the geometry optimization of the molecules.

Theoretical aspects: In present study, various parameters associated with the overall chemical reactivity of the molecules were investigated. In general, the chemical reactivity for a molecule or complex can be expressed by a collection of reactivity parameters like chemical potential, ionization potential, electron affinity, chemical hardness, chemical softness, electrophilic index, nucleophilic index, *etc.* [18]. The investigation of computed value of these parameters can be achieved by the application of the Frontier molecular orbital (FMO) theory [19].

The global reactivity indices can collectively reveal the structural characteristics, chemical reactivity and respective bonding opportunities present during the course of the reaction. In general, global reactivity parameters are an indicator of the overall chemical behaviour of a molecule. Ionization potential (IP) represents the energy required to remove an electron from the highest occupied molecular orbital of the complex [20]. This parameter plays a significant role in predicting the complex's ability to donate electrons and participate in redox reactions. Further, ionization potential can be simply expressed by Koopman's approximation (eqn. 1), which states that the ionization potential is negative of the energy of highest occupied molecular orbital (E_{HOMO}) [21]. In contrast, electron affinity (EA) assesses the reactivity of a molecule or complex to an extra electron [20]. Mathematically, electron affinity can also be determined by Koopman's approximation (eqn. 2), which states that electron affinity is the negative of the energy of the lowest unoccupied molecular orbital (E_{LUMO}).

Further, the tendency of the electron cloud to escape from the molecule is measured by the chemical potential (μ), which is equivalent to the opposite of the electronegativity χ (tendency to attract a shared pair of electron), as delineated by Pauling & Mulliken [22-24]. A simple approximation between IP and EA can be employed in order to compute the electronegativity (χ) and chemical potential (μ) can be expressed in eqns. 3 and 4, respectively.

Furthermore, in order to calculate the hardness (η) of the molecule/complex, the function defined by Parr & Pearson, was also employed (eqn. 5) [22]. Briefly, chemical hardness is a measure of the resistance of a metal-ligand complex to electron density changes when it interacts with other molecules or undergoes chemical reactions. Generally, it can be derived from the chemical potential's first derivative, with N under the constraint of a fixed external potential. On the other hand, softness (S) is a quantitative measure of the amount of electron cloud diffused from the molecule and is mathematically expressed as the reciprocal of hardness (η) [23].

Further, according to Pearson's theory of acids and bases, both hardness (η) and softness (S) can be expressed in terms of the ionization potentials (IP) and electron affinity (EA) [25]. The mathematical expressions are shown in eqn. 6 respectively.

$$IP = -E_{HOMO} \quad (1)$$

$$EA = -E_{LUMO} \quad (2)$$

$$\chi = \frac{(\text{IP} + \text{EA})}{2} \quad (3)$$

$$\mu = -\chi \quad (4)$$

$$\eta = \left(\frac{\partial \mu}{\partial N} \right) = \frac{1}{S} \quad (5)$$

$$\eta = \frac{(\text{I} - \text{A})}{2} = \frac{1}{S} \quad (6)$$

In addition to chemical hardness and softness, another important parameter that can be evaluated using density functional theory is the electrophile index (ω). The electrophile index provides information about the ability of a molecule to act as an electrophile, or electron acceptor, in chemical reactions. Parr and coworkers have defined electrophilicity index as a function of chemical potential and hardness. In general, electrophile index (ω), can be determined using the mathematical formula as expressed in eqn. 7 [26,27]. On the other hand, nucleophilicity index (NI) is a measure of the nucleophilic behaviour of a molecule or complex, indicating its tendency to donate a pair of electrons to form a new chemical bond. Mathematically, NI is negative value of the ionization potential and usually expressed as shown in eqn. 8 [26].

$$\omega = \frac{\mu^2}{2\eta} \quad (7)$$

$$\text{NI} = -\text{IP} \quad (8)$$

RESULTS AND DISCUSSION

Theoretical studies of ligand and their metal complexes:

Theoretical investigation was performed on the metal complexes of ligand MEC to explore the interactions and complexation behaviour of the ligand MEC with metal ions. Firstly, the complexes initial geometry was optimized using the molecular mechanics (MM) approach and followed by reoptimization employing semi-empirical method using PM6 parameter [28]. Further, in order to obtain the final geometries of the complexes with least strain energy structures, the optimized structures were again optimized using the density functional theory (DFT) approach [29]. The complexes were examined using

frequency calculations, where the absence of imaginary frequencies indicated that the geometry of the molecules was entirely optimized and provided confirmation of the energy minima for the geometry. All the calculations were carried out for the complexes in the gas phase only. Fig. 2 represents the optimized structures for complexes consists of ligand MEC and trivalent metal ion complexes Al^{3+} , Cr^{3+} and Fe^{3+} , respectively. Further, the energies of the optimized structures for ligand MEC with trivalent metal ion complexes Al^{3+} , Cr^{3+} and Fe^{3+} , respectively were calculated using DFT and found to be -1484.708 a.u., -1567.51 a.u. and -2746.328 a.u., respectively.

Thermodynamic parameters and relative stability: In order to access the overall stability of metal-ligand complex, the thermodynamic parameters *viz.* enthalpy, entropy and Gibbs free energy, for the ligand MEC with trivalent metal ion Al^{3+} , Cr^{3+} and Fe^{3+} complexes employing DFT method were calculated. All the parameters were calculated in the gaseous phase and indicates the order of stability of the complexes. The results (Table-1) revealed that the lowest value of enthalpy for MEC- Fe^{3+} complex (-2745.90 a.u.), followed by MEC- Cr^{3+} (-1567.11 a.u.) and highest value for MEC- Al^{3+} (-1484.28 a.u.) complexes respectively. Further, the Gibbs free energy follows the trend as MEC- Fe^{3+} (-2745.99 a.u.) < MEC- Cr^{3+} (-1567.19 a.u.) < MEC- Al^{3+} (-1484.37 a.u.), respectively. These data sets clearly indicate towards the better stability of ligand MEC to complex Fe^{3+} metal ion among all three metal ions under consideration. A comparative graphical representation of thermodynamic parameters is shown in Fig. 3.

TABLE-1
THERMODYNAMIC PARAMETERS *viz.* ENTHALPY (H), ENTROPY (S) AND GIBBS FREE ENERGY (G) CALCULATED BY USING DENSITY FUNCTIONAL THEORY WITH B3LYP PARAMETER FOR MEC- Al^{3+} , MEC- Cr^{3+} AND MEC- Fe^{3+} COMPLEXES, RESPECTIVELY

Complexes	H (a.u.)	G (a.u.)	S (cal/mol)
MEC- Al^{3+}	-1484.28	-1484.37	183.95
MEC- Cr^{3+}	-1567.11	-1567.19	182.37
MEC- Fe^{3+}	-2745.90	-2745.99	181.78

Frontier molecular orbitals (FMO) calculation: In order to calculate the energies of frontier molecular orbitals *i.e.* highest occupied molecular orbital (HOMO) and lowest unoccupied

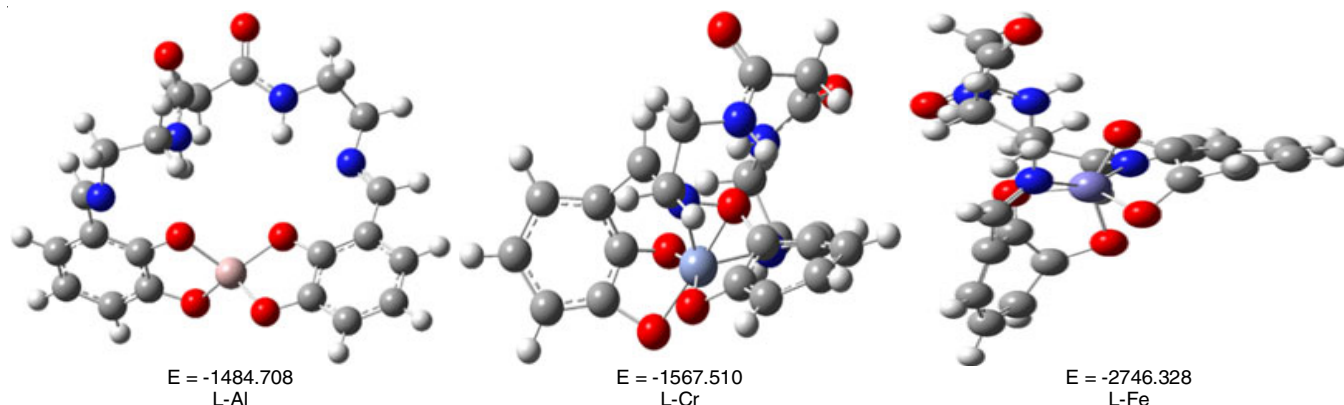


Fig. 2. Schematic representation of the optimized structures of the ligand-metal complexes by using DFT/B3LYP: (a) MEC- Al^{3+} , (b) MEC- Cr^{3+} and (c) MEC- Fe^{3+} , respectively

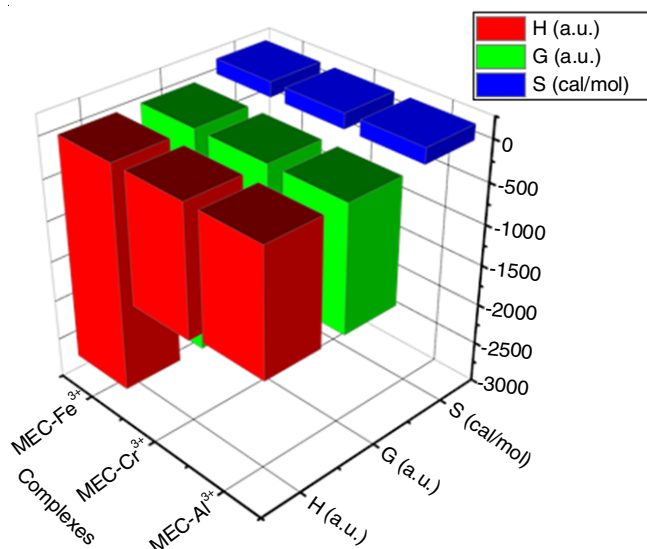


Fig. 3. A comparative graphical analysis of major thermodynamic parameters *viz.* enthalpy (H), entropy (S) and Gibbs free energy (G) calculated by using density functional theory with B3LYP parameter for of MEC- Al³⁺, MEC-Cr³⁺ and MEC-Fe³⁺ metal complexes, respectively

molecular orbital (LUMO) for all the metal complexes *viz.* MEC-Al³⁺, MEC-Cr³⁺ and MEC-Fe³⁺, we have employed TD-DFT calculations using B3LYP hybrid functional. Further, the relative energy gap between HOMO and LUMO were calculated for all three metal complexes with the help of the respective energies of HOMO and LUMO.

The calculated values of energies of HOMO and LUMO with respective ΔE values (relative energy gap between HOMO and LUMO) for MEC-Al³⁺, MEC-Cr³⁺ and MEC-Fe³⁺ complexes are shown in Table-2. Further, a comparative graphical analysis of corresponding HOMO and LUMO with their respective band gap for MEC-Al³⁺, MEC-Cr³⁺ and MEC-Fe³⁺ complexes are presented in Fig. 4. It was found that the energy gap ($\Delta E = 2.29$ eV) is the minimum for MEC-Cr³⁺ complex which suggests the most reactive nature of this complex among all three complexes. On the other hand, MEC-Al³⁺ complex exhibits the highest value of ΔE (4.24 eV), reflecting towards its least reactive behaviour among all three metal-ligand complexes under consideration.

Complexes	E_{HOMO} (eV)	E_{LUMO} (eV)	ΔE (eV)
MEC-Al ³⁺	-2.99	1.25	4.24
MEC-Cr ³⁺	-2.61	-0.33	2.29
MEC-Fe ³⁺	-5.99	-0.123	3.35

In general, organic semiconductor materials show band gap in the range of ~ 1- 5 eV. Here, all three metal–ligand complexes fall in the same range and can exhibits potential applications in a range of semi-conductivity based applications [30]. Further, we have explored the relative electron density distribution for all trivalent metal-ligand complexes employing DFT based B3LYP/LANL2DZ functionals. The relative electron

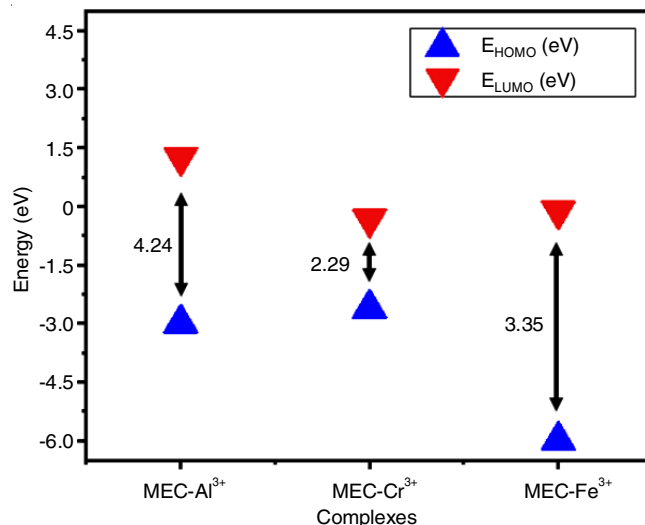


Fig. 4. Calculated band gap (difference in energies between HOMO and LUMO) of the MEC-Al³⁺, MEC-Cr³⁺ and MEC-Fe³⁺ complexes, respectively

energy distribution can access possible location of HOMO and LUMO electron density at the specific atomic center in the molecule. Fig. 5 demonstrates the HOMO and LUMO electron density distribution for all trivalent metal complexes. After careful observation of the structures in Fig. 5, it can be inferred that HOMO and LUMO electron density are mainly located on the binding unit *i.e.* catechol moiety and the central metal atom of the complexes except the LUMO molecular orbital of MEC-Al³⁺ where the electron density is shifted to the central unit of the complex *i.e.* the amide part of the complex. In general, the location of the HOMO and LUMO electron density can help us to predict the behaviour of the specific sites as

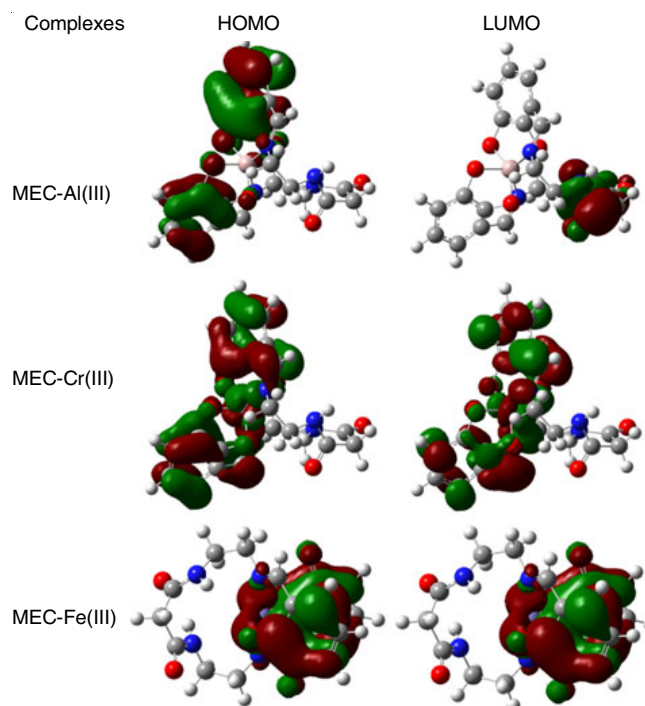


Fig. 5. Frontier molecular orbitals of the ligand-metal complexes by using DFT/B3LYP/LANL2DZ

electrophile or nucleophile. In most of the cases, the localization of the HOMO electron density can be associated with the ease of electron participation in the reaction and that specific site can behave as nucleophile. On the other hand, the location of LUMO electron density can be associated with the presence of good electrophilic site [31].

Global indices of reactivity: In a general sense, the chemical reactivity of a molecule or complex can be expressed by a collection of chemical potential, ionization potential, electron affinity, chemical hardness, chemical softness, electrophilic index and nucleophilic index, amongst others [26]. Since the molecular orbital approach, which is based on the wave function, typically yields extremely accurate findings, its applicability is limited by the interference of related correlation effects and the need for an excessively complex computing setup [32]. Density functional theory offers another route for methodically examining the reactivity parameters. It operates on the basis of electron density for the computation of all ground state information [17]. Further, the reactive parameters were calculated as derivative of electron density and total energy, therefore the dependency on the spatial and spin coordinates of all the electrons in the molecules are no longer a problem [27]. A relative comparison of all these reactive parameters for MEC-Al³⁺, MEC-Cr³⁺ and MEC-Fe³⁺ complexes are shown in Table-3.

From Table-3, the value of IP value for MEC-Cr³⁺ complex is 2.61 eV, which is lowest among all three metal-ligand complexes, suggest greater tendency of MEC-Cr³⁺ complex to exhibits electron removal among all three metal-ligand complexes. On the other hand, MEC-Fe³⁺ complex exhibits IP value of 5.99 eV, which is highest among all, suggests its least ease of electron removal behaviour among all metal-ligand complex. Thus, three metal-ligand complex in an increasing order of their IP as MEC-Cr³⁺ < MEC-Al³⁺ < MEC-Fe³⁺. In contrary to IP observation, EA will follows the reverse trend. It was found that the order of EA is MEC-Al³⁺ < MEC-Fe³⁺ < MEC-Cr³⁺ respectively. Lower the value of electronegativity, lesser is the tendency to donate electrons.

Further, in order to access the feasible interaction of the metal ligand complex with other reactive species, the electronegativity and chemical potential are among the most important reactivity descriptors [20]. In general, electronegativity is the tendency of the complex to attract a shared pair of electrons towards it. On the other hand, chemical potential can be related to escaping nature of the electron cloud [33]. From Table-3, it is found that MEC-Fe³⁺ having the highest value of electronegativity *i.e.* 4.68 eV, which suggests that it is more electrophilic than other metal-ligand complexes under investigation. On the other hand, MEC-Al³⁺ exhibits lowest value of electronegativity *i.e.* 0.87 eV, indicating towards its lesser electrophile

behaviour among all metal-ligand complex. On the contrary, the chemical potential follows the reverse trend *i.e.* MEC-Fe³⁺ < MEC-Cr³⁺ < MEC-Al³⁺. According to this, MEC-Al³⁺ can exhibits the highest tendency to escape the electron cloud among all three metal-ligand complex under investigation.

Further, it is interesting to observe that higher the electronegativity of complex, greater is its tendency to exhibits electrophilic nature. In other words, higher the electronegativity, higher will be the value of electrophilicity index (EI) [34]. Therefore, electrophilic index will follow the same trend as that of electronegativity *i.e.* MEC-Al³⁺ < MEC-Cr³⁺ < MEC-Fe³⁺, respectively. This shows that MEC-Fe³⁺ complex is most electrophilic among all with a electrophilic index value of 8.38, on the other hand, MEC-Al³⁺ is the least electrophilic among all with a electrophilic value of 0.18 respectively.

On the other hand, nucleophilicity index (NI) follows the other trends *i.e.* MEC-Fe³⁺ < MEC-Al³⁺ < MEC-Cr³⁺ respectively. Interestingly, MEC-Cr³⁺ complex exhibits highest value of nucleophilic index *i.e.*, -2.61 among all, indicating its greater nucleophilic behaviour in the reactions. On the other hand, MEC-Fe³⁺ have shown lowest nucleophilic value *i.e.*, -5.99 among all, which indicates towards least nucleophilic behaviour among all metal-ligand complexes under investigation.

The hardness of the metal complex can be defined as the variation of chemical potential with N under constraint of a fixed external potential [18]. After careful analysis of Table-3, it was found that MEC-Al³⁺ exhibits highest value of hardness *i.e.* 2.12, indicating towards its greater stability towards the chemical reactions among all three studied metal-ligand complexes. On the other hand, MEC-Cr³⁺ complex exhibits lowest value of hardness *i.e.* 0.76, which suggests that MEC-Cr³⁺ complex is more reactive among all three metal-ligand complexes under consideration.

In general, the energy difference between the HOMO and LUMO states, also known as the band gap and the hardness and softness of a compound are connected with one another. Mostly, it has been observed that larger energy gaps make compounds more resistant to the process of charge transfer, owing to their more stability, more hardness and less reactive nature. In reference to present investigation, the common trend for energy gap, hardness and stability of the metal-ligand complexes follows the order: MEC-Cr³⁺ < MEC-Fe³⁺ < MEC-Al³⁺ respectively. On the other hand, the common trend for reactivity and softness of the metal-ligand complexes follows the order MEC-Al³⁺ < MEC-Fe³⁺ < MEC-Cr³⁺, respectively.

Molecular electrostatic potential surface (MEPs): Fig. 6 demonstrates the molecular electrostatic potential (MEP) surfaces for all three metal-ligand complexes. The molecular electrostatic potential surface, which is helpful in detecting

TABLE-3
RELATIVE COMPARISON OF GLOBAL REACTIVITY PARAMETERS INDICES CALCULATED BY EMPLOYING CONCEPTUAL DENSITY FUNCTIONAL THEORY FOR MEC-Al³⁺, MEC-Cr³⁺ AND MEC-Fe³⁺ COMPLEXES, RESPECTIVELY

Complexes	IP (eV)	EA (eV)	μ (eV)	χ (eV)	η (eV)	S (eV)	ω (eV)	N.I.
MEC-Al ³⁺	2.99	-1.25	-0.87	0.87	2.12	0.47	0.18	-2.99
MEC-Cr ³⁺	2.61	0.33	-1.47	1.47	1.14	0.88	0.94	-2.61
MEC-Fe ³⁺	5.99	0.123	-4.68	4.68	1.31	0.76	8.38	-5.99

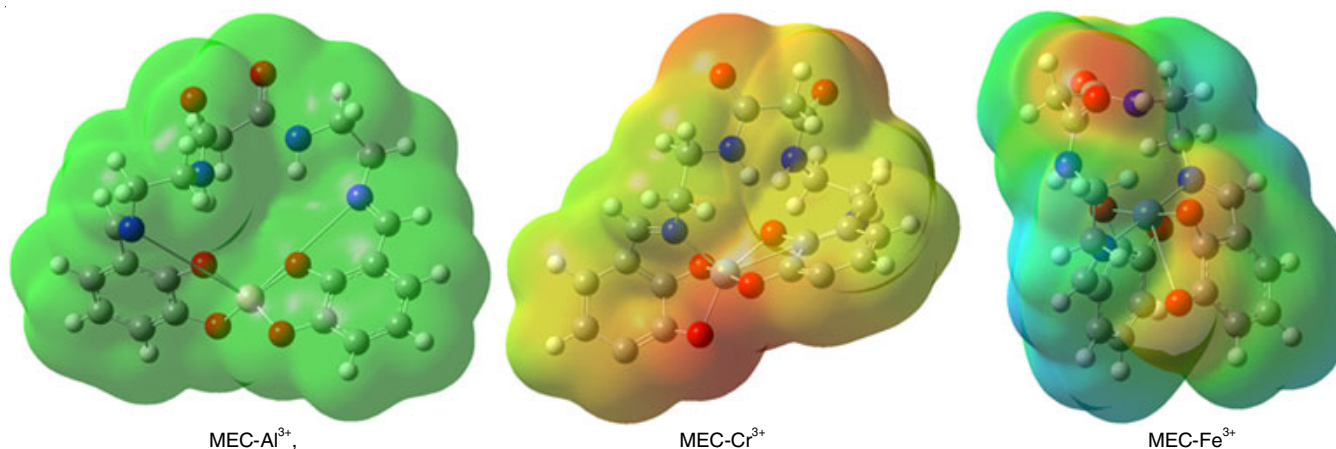


Fig. 6. Representative images of molecular electrostatic potential (MEP) surfaces MEC-Al³⁺, MEC-Cr³⁺ and MEC-Fe³⁺ complexes, respectively

the region of electrophilic and nucleophilic assault, is utilized in order to identify the regions of the system that are particularly abundant in electrons and those that are lacking in electrons [35]. On the surface of molecular electrostatic potential (MEP), a zone of high electron density is indicated by the colour red. This zone is associated with a negative electrostatic potential, while the colour blue is associated with a zone of high electron density, which is associated with a positive electrostatic potential [36]. The green colour, which denotes zero electrostatic potential, represents the neutral region. The fact that the green region is present on each and every atom in the aluminium complex is evidence that the electrostatic potential of the molecule is identical to zero.

On the other hand, the red hue of the oxygen atoms in the chromium complex indicates that the oxygen atoms have a high electron density, while the carbon and hydrogen atoms have a low electron density, respectively. Additionally, the oxygen atoms in the iron complex have red regions, the nitrogen atoms have blue regions and the carbon and hydrogen atoms have green regions. All of these regions are contained within the iron complex. Electron-rich density is largely observed on heteroatoms, such as oxygen and nitrogen atoms, in all of the complexes that are being investigated, whereas electron-deficient sites are found on carbon and hydrogen atoms.

Conclusion

In present study, we have carried out the DFT, TD-DFT and conceptual DFT based analysis for the investigation of thermodynamic and chemical reactivity parameters of MEC-Al³⁺, MEC-Cr³⁺ and MEC-Fe³⁺ complexes (where MEC = N₁,N₃-bis(2-(((Z)-2,3-dihydroxybenzylidene)amino)ethyl)-malonamide)). On the basis of DFT analysis for calculation of the energy, thermodynamic and electronic properties, it was found that the MEC-Fe³⁺ complex is more stable than the Al³⁺ and Cr³⁺ complexes. Additionally, the MEC-Fe³⁺ complex appeared to be more stable thermodynamically due to minimal value of Gibbs free energy *i.e.* $G = -2745.99$. Further, on the basis of conceptual DFT analysis, the MEC-Cr³⁺ complex appeared to be more reactive and more soft among all metal-ligand complexes under consideration.

CONFLICT OF INTEREST

The authors declare that there is no conflict of interests regarding the publication of this article.

REFERENCES

- M.K. Abd Elnabi, N.E. Elkaliny, M.M. Elyazied, S.H. Azab, S.A. Elkhalfifa, S. Elmasry, M.S. Mouhamed, E.M. Shalamesh, N.A. Alhoriény, A.E. Abd Elaty, I.M. Elgendy, A.E. Etman, K.E. Saad, K. Tsigkou, S.S. Ali, M. Kornaros and Y.A.-G. Mahmoud, *Toxics*, **11**, 580 (2023); <https://doi.org/10.3390/toxics11070580>
- M. Balali-Mood, K. Naseri, Z. Tahergorabi, M.R. Khazdair and M. Sadeghi, *Front. Pharmacol.*, **12**, 643972 (2021); <https://doi.org/10.3389/fphar.2021.643972>
- T. Arao, S. Ishikawa, M. Murakami, K. Abe, Y. Maejima and T. Makino, *Paddy Water Environ.*, **8**, 247 (2010); <https://doi.org/10.1007/s10333-010-0205-7>
- J.W. Eaton and M. Qian, *Free Radic. Biol. Med.*, **32**, 833 (2002); [https://doi.org/10.1016/S0891-5849\(02\)00772-4](https://doi.org/10.1016/S0891-5849(02)00772-4)
- G. Papanikolaou and K. Pantopoulos, *Toxicol. Appl. Pharmacol.*, **202**, 199 (2005); <https://doi.org/10.1016/j.taap.2004.06.021>
- R.M. Saaltink, S.C. Dekker, M.B. Eppinga, J. Griffioen and M.J. Wassen, *Plant Soil*, **416**, 83 (2017); <https://doi.org/10.1007/s11104-017-3190-4>
- C. Exley, *Morphologie*, **100**, 51 (2016); <https://doi.org/10.1016/j.morpho.2015.12.003>
- M. Closset, K. Cailliau, S. Slaby and M. Marin, *Int. J. Mol. Sci.*, **23**, 31 (2021); <https://doi.org/10.3390/ijms23010031>
- R.W. Gensemer and R.C. Playle, *Crit. Rev. Environ. Sci. Technol.*, **29**, 315 (1999); <https://doi.org/10.1080/10643389991259245>
- M. Costa and C.B. Klein, *Crit. Rev. Toxicol.*, **36**, 155 (2006); <https://doi.org/10.1080/10408440500534032>
- S.R. Shelnutt, P. Goad and D.V. Belsito, *Crit. Rev. Toxicol.*, **37**, 375 (2007); <https://doi.org/10.1080/10408440701266582>
- M. Jaishankar, T. Tseten, N. Anbalagan, B.B. Mathew and K.N. Beeregowda, *Interdiscip. Toxicol.*, **7**, 60 (2014); <https://doi.org/10.2478/intox-2014-0009>
- M.S. More, P.G. Joshi, Y.K. Mishra and P.K. Khanna, *Mater. Today Chem.*, **14**, 100195 (2019); <https://doi.org/10.1016/j.mtchem.2019.100195>
- L.H. Abdel-Rahman, M.T. Basha, B.S. Al-Farhan, W. Alharbi, M.R. Shehata, N.O. Al Zamil and D. Abou El-ezz, *Molecules*, **28**, 4777 (2023); <https://doi.org/10.3390/molecules28124777>

15. A. Amardeep, V. Dangi, P. Kumar, M. Meenakshi, M. Baral, B. Arya and T. Sheoran, *Orient. J. Chem.*, **40**, 274 (2024); <https://doi.org/10.13005/ojc/400133>
16. B.J. Duke and B. O'Leary, *J. Chem. Educ.*, **69**, 529 (1992); <https://doi.org/10.1021/ed069p529>
17. Y.C. Xu, N. Li, X. Yan and H.X. Zou, *Environ. Sci. Pollut. Res. Int.*, **30**, 91780 (2023); <https://doi.org/10.1007/s11356-023-28854-6>
18. R. Pal and P.K. Chattaraj, *J. Indian Chem. Soc.*, **98**, 100008 (2021); <https://doi.org/10.1016/j.jics.2021.100008>
19. J. Yu, N.Q. Su and W. Yang, *JACS Au*, **2**, 1383 (2022); <https://doi.org/10.1021/jacsau.2c00085>
20. C.G. Zhan, J.A. Nichols and D.A. Dixon, *J. Phys. Chem. A*, **107**, 4184 (2003); <https://doi.org/10.1021/jp0225774>
21. R. Shankar, K. Senthilkumar and P. Koldaivel, *Int. J. Quantum Chem.*, **109**, 764 (2009); <https://doi.org/10.1002/qua.21883>
22. J.L. Gázquez, in eds.: K.D. Sen, *Hardness and Softness in Density Functional Theory*, In: *Chemical Hardness. Structure and Bonding*, Springer-Verlag: Berlin/Heidelberg, vol. 80, pp. 27-43 (1993).
23. H. Xu, D.C. Xu and Y. Wang, *ACS Omega*, **2**, 7185 (2017); <https://doi.org/10.1021/acsomega.7b01039>
24. M. Franco-Pérez and J.L. Gázquez, *J. Phys. Chem. A*, **123**, 10065 (2019); <https://doi.org/10.1021/acs.jpca.9b07468>
25. P.W. Ayers, M. Mohamed and F. Heidar-Zadeh, in eds.: S. Liu, *The Hard/Soft Acid/Base Rule: A Perspective from Conceptual Density Functional Theory*, In: *Conceptual Density Functional Theory: Towards a New Chemical Reactivity Theory*, Wiley; vol. 2, pp. 263-279 (2022).
26. L. Domingo, M. Ríos-Gutiérrez and P. Pérez, *Molecules*, **21**, 748 (2016); <https://doi.org/10.3390/molecules21060748>
27. D. Chakraborty and P.K. Chattaraj, *Chem. Sci.*, **12**, 6264 (2021); <https://doi.org/10.1039/D0SC07017C>
28. P.V. Bernhardt and P. Comba, *Inorg. Chem.*, **31**, 2638 (1992); <https://doi.org/10.1021/ic00038a060>
29. W. Wang, J. Zhu, Q. Huang, L. Zhu, D. Wang, W. Li and W. Yu, *Molecules*, **29**, 308 (2024); <https://doi.org/10.3390/molecules29020308>
30. R.E. Aderne, B.G.A.L. Borges, H.C. Ávila, F. Von Kieseritzky, J. Hellberg, M. Koehler, M. Cremona, L.S. Roman, C.M. Araujo, M.L.M. Rocco and C.F.N. Marchiori, *Mater. Adv.*, **3**, 1791 (2022); <https://doi.org/10.1039/D1MA00652E>
31. L. Domingo, *Molecules*, **21**, 1319 (2016); <https://doi.org/10.3390/molecules21101319>
32. R.D. Hancock, *Acc. Chem. Res.*, **23**, 253 (1990); <https://doi.org/10.1021/ar00176a003>
33. R.J. Bartlett, I. Grabowski, S. Hirata and S. Ivanov, *J. Chem. Phys.*, **122**, 034104 (2005); <https://doi.org/10.1063/1.1809605>
34. P. Pérez, L.R. Domingo, A. Aizman and R. Contreras, *Theor. Comput. Chem.*, **19**, 139 (2007); [https://doi.org/10.1016/S1380-7323\(07\)80010-0](https://doi.org/10.1016/S1380-7323(07)80010-0)
35. A. Daolio, A. Pizzi, M. Calabrese, G. Terraneo, S. Bordignon, A. Frontera and G. Resnati, *Angew. Chem. Int. Ed.*, **60**, 20723 (2021); <https://doi.org/10.1002/anie.202107978>
36. S. Kenouche, C. Sandoval-Yañez and J.I. Martínez-Araya, *Chem. Phys. Lett.*, **801**, 139708 (2022); <https://doi.org/10.1016/j.cplett.2022.139708>